JOURNAL OF GUIDANCE, CONTROL, AND DYNAMICS
Vol. 30, No. 2, March–April 2007

Classification of the Distant Stability Regions at Europa

Martin Lara*
Real Observatorio de la Armada, 11110 San Fernando, Spain
and
Ryan Russell† and Benjamin Villac‡
Jet Propulsion Laboratory, California Institute of Technology, Pasadena, California 91109-8099

DOI: 10.2514/1.22372

Long-term stable trajectories around Europa, one of the Galilean moons of Jupiter, are analyzed for their potential applications in spacecraft trajectory design, such as end-of-mission disposal options, backup orbits, or intermediary targets for transfer trajectories. The phase space is analyzed via the computation of families of periodic orbits and the estimation of their stability character. Although the core analysis of the paper uses the circular restricted three-body problem, a selected set of long-term stable solutions is checked by integrating the corresponding initial conditions in an ephemeris model over several years. The current model and methods can be readily applied to other planetary satellites including the other Galileans at Jupiter, the many satellites at Saturn, and the Earth's moon.

Introduction

THE design of space missions with close-range analysis of potentially life-harboring celestial bodies is generally constrained by planetary protection measures. Such requirements directly result in constraints on lifetime and recovery margins to be taken into account in the design of the spacecraft trajectory. For example, nonimpact conditions with a celestial body must not only be satisfied for the nominal trajectory under nominal hardware conditions but must also encompass the evolution of the spacecraft in the event of missed thrust or other problems with the propulsion system. In the worst case scenario, a complete loss of thrust during a maneuver may result in placing the spacecraft in an unstable environment from which the nominal course of the mission may be difficult, or impossible, to recover.

Stable-periodic and quasi-periodic trajectories can be used to achieve such goals because the natural dynamics do not lead a spacecraft into risky episodes. Indeed, such trajectories are grouped in extended regions of phase space with similar qualitative characteristics to form stability regions [1] so that a missed thrust or maneuver opportunity starting from such regions will require one to wait only a few periods before new opportunities can be found.

Although the characterization and discussion of the stability properties of an orbiter close to Europa has been considered in several papers [2–6], the exploration of more distant stable regions has received much less attention, except for the case of distant retrograde orbits (DRO) [1,7,8]. This research has shown that, in the case of DROs, the stability regions present very strong stability properties but are also surrounded by very unstable motion and may disappear in certain regions of phase space. In particular, it is not clear if other options are available besides the DRO regions and what are the qualitative characteristics of these other stability regions. This problem thus involves the determination of the existence of distinct types of stability regions and the potential connections among them as well as the characterization of the different classes. The present paper aims to explore the first part of this problem by classifying the main stability regions via the computation of stable periodic orbit families. Low-order periodic orbits indeed form a sort of backbone of the stability regions around which other similar periodic and quasi-periodic stable trajectories organize themselves. The results compounded in this paper thus indicate the existing stability regions available to a spacecraft trajectory mission designer. Some further characterizations of the stability regions reported in this paper can be found in [9] and will be reported more fully in a subsequent paper.

The approach taken uses the circular restricted three-body problem (CRTBP) to model the underlying dynamics and aims at computing families of periodic orbits that bifurcate from the main planar families. A brief indication of the long-term stability properties of the class of solutions reported is discussed and illustrated by the evaluation of a selected set of trajectories in an ephemeris system. While the qualitative types of families of periodic orbits reported have been considered in many studies in the field of astronomy and celestial mechanics, the results appear to be scattered in a large literature with no relation to the problem considered here. Besides offering a summary of these scattered results in a form usable for a spacecraft trajectory mission designer, this paper presents quantitative results for a specific system of interest to future science missions, the Jupiter–Europa system. Finally, the method used for classifying the regions of long-term stability appears to be systematic and, thus, applicable to other systems of interest, such as the Earth–moon system or any of the systems associated with the gas giants. All of these contributions are useful for the practicing engineers.

After a brief review of the CRTBP dynamics, the paper proceeds to the computation and description of the different families of periodic orbits. Finally, a discussion on the different classes of long-term stability solutions and an evaluation of their robustness to perturbation in a more realistic model than the CRTBP is given.

Dynamical Model

We assume that Jupiter and Europa revolve in circular orbits around their mutual center of mass. In a synodic system with the origin at Europa and Jupiter on the negative x axis, the nondimensional equations of motion of the CRTBP are

$$\ddot{x} - 2\dot{y} = \Omega_x, \qquad \ddot{y} + 2\dot{x} = \Omega_y, \qquad \ddot{z} = \Omega_z \tag{1}$$

where the potential function is

Presented at the 2005 AAS/AIAA Astrodynamics Specialist Conference, Lake Tahoe, California, 7–11 August 2005; received 10 January 2006; revision received 21 April 2006; accepted for publication 10 May 2006.

*Commander, Ephemeris Section; mlara@roa.es.
†Engineer, Guidance, Navigation and Control Section, Mail Stop 301-140L, 4800 Oak Grove Drive; Ryan.Russell@jpl.nasa.gov.
‡Engineer, Guidance, Navigation and Control Section, Mail Stop 301-140L, 4800 Oak Grove Drive; currently Professor, Mechanical and Aerospace Engineering, University of California, Irvine, 4200 Engineering Gateway, Irvine, CA 92697-3975; bvillac@uci.edu.

$$\Omega = \frac{1}{2}[(x+1-\mu)^2 + y^2] + \frac{1-\mu}{\rho} + \frac{\mu}{r} \tag{2}$$

and ρ and r are the distances to Jupiter and Europa, respectively,

$$\rho^2 = (x+1)^2 + y^2 + z^2, \qquad r^2 = x^2 + y^2 + z^2 \tag{3}$$

(Units of mass, length, and time are chosen as the total mass of the system, the distance from Jupiter to Europa, and the system period divided by 2π, respectively.) Changing the barycentric origin is done by simply adding $1-\mu$ to the coordinate x. In our computations, we use normalizing units of length and time. In these units $\mu = 2.528 \times 10^{-5}$, and the equatorial radius of Europa is $r_E = 2.334 \times 10^{-3}$.

The equatorial plane defined by $z = \dot{z} = 0$ is invariant under the equations of motion, thus allowing us to talk about planar motion. These dynamics also accept the Jacobi integral of motion:

$$\mathcal{J} \equiv 2\Omega(x, y, z) - (\dot{x}^2 + \dot{y}^2 + \dot{z}^2) = C \tag{4}$$

where C is the Jacobi constant. This constant represents a natural parameter for families of periodic orbits.

Although the CRTBP represents a significant simplification over most accurate models for the Jupiter–Europa environment, in particular, with respect to very long-term or asymptotic motion [10], the sets of trajectories of interest in this paper should be, by definition, robust to small perturbations and thus continue to exist in the CRTBP. The choice of this model for our analysis has the advantage of resulting in numerical integration routines faster than those needed to integrate high-fidelity models and represents an autonomous Hamiltonian approximation to the dynamics (availability of an integral of motion) that simplifies the analysis in some cases. A full description of the CRTBP can be found in specialized books such as [11].

Stability Analysis via Periodic Orbits: Background and Method

As noted in the introduction, periodic orbits form a backbone to the dynamics of the CRTBP. Henri Poincaré even conjectured at the beginning of the 20th century that the set of periodic orbits is dense in phase space. From a numerical viewpoint, this conjecture imposes itself as a practical issue as periodicity conditions are determined only with a finite accuracy: a nonperiodic recurrent trajectory will appear as a high-order periodic orbit from a numerical perspective. In particular, this is the case for stable quasi-periodic orbits, where the numerical evaluation of the stability properties of higher-order bifurcated families allows us to estimate the existence of connected stability regions. Further, as the linear stability character of such families is a by-product of the corrector–predictor scheme used to compute the families, the bifurcated families of periodic orbits offer a basic structure upon which to classify the long-term stability regions.

Linear Stability and Bifurcations

The stability of a periodic orbit is conceived from the behavior of the periodic orbit variations. Therefore, the variational equations must be integrated for every periodic orbit of interest. The first-order variations conform a linear differential system with periodic coefficients. As we know from Floquet's theory, its general solution is made of a linear combination of exponentials $e^{\alpha t}$ (or *characteristic multipliers*) whose coefficients are not constant but contain periodic solutions with the same period T of the periodic orbit. Therefore, to determine the stability behavior of a periodic orbit (in linear approximation) it is enough to study the multipliers at the end of one period $\lambda = e^{\alpha T}$ (or the eigenvalues λ of the *monodromy* matrix).

The CRTBP is a Hamiltonian problem, therefore, the eigenvalues appear in reciprocal pairs $(\lambda, 1/\lambda)$. Further, periodic orbits enjoy one trivial eigenvalue $\lambda_0 = 1$ that, for Hamiltonian systems, has a multiplicity of 2. Then, periodic orbits of Hamiltonian systems with 3 degrees of freedom have four nontrivial eigenvalues, and two stability indices are normally used [12]

$$b_i = \lambda_i + 1/\lambda_i \qquad i = 1, 2 \tag{5}$$

The condition b_i real and $|b_i| < 2$ $(i = 1, 2)$ applies for linear stability.

When dealing with planar motions, one index measures the "horizontal" or in-plane stability (that we denote b_h), whereas the other (denoted b_v) shows the "vertical" stability character of the periodic orbit [13], that is the orbit's behavior when undergoing perturbations in the out-of-plane direction. There are critical values of the stability indices (some nontrivial eigenvalues taking the value $\lambda = \pm 1$) where new families of periodic orbits can bifurcate from the original one, either in the plane (critical horizontal index $b_h = \pm 2$) or orthogonal to it (critical vertical index $b_v = \pm 2$).

Note that $b = +2 \Rightarrow \lambda = +1$, and the bifurcation occurs with the same period of the critical orbit. The case $b = -2$ implies that $\lambda = -1$ and $\lambda^2 = e^{\alpha(2T)} = 1$ resulting in a period doubling bifurcation. Besides the critical cases $b = \pm 2$, for $-2 < b < 2$ other families of periodic orbits may bifurcate with multiple period from the original one [14] (see also [15,16]). Thus, for eigenvalues λ that are nth roots of the unity $\lambda = \cos(2\pi d/n) + j\sin(2\pi d/n)$ and

$$b = 2\cos(2\pi d/n) \tag{6}$$

where d and n are integer numbers and j is the imaginary unit, the corresponding stability index of the n-fold periodic orbit, the T-periodic orbit after a period $\tau = nT$, is $b = +2$. We call these critical orbits "d:n-resonant orbits" and the families of periodic orbits that emerge from a d:n-resonant orbit "d:n-resonant families."

Families, Stability Curves, and Stability Regions

Given a periodic orbit, the smooth variation of one of its characteristics results in a smooth set of periodic orbits known as families. One typical parameter is the Jacobi constant, leading to the notion of natural family [17]. As the parameter is varied, the stability properties of the periodic orbits vary accordingly, and the representation of the stability indices versus the parameter or integral generator of a family of periodic orbits produce what Hénon calls "stability curves" [14], where the changes in the stability of a family can be clearly appreciated. The stability curves are usually represented in the real plane. However, unstable orbits with complex eigenvalues out of the unit circle have complex stability indices. Therefore, in some cases we use 3-D stability curves. For a detailed description of the different cases of instability that can appear, the interested reader is referred to advanced textbooks on the topic or to the original reference [12].

There exist a great variety of families of periodic orbits of the CRTBP. However, because we are mainly interested in orbits enjoying long-term stability, we pay special attention to the family of equatorial retrograde orbits around Europa (hereafter, "the retrograde family") without limiting to the DROs case of [7,8]. Also of high interest is the "direct family" of equatorial direct orbits around Europa, providing large regions of orbit stability for almost circular and egg-shaped orbits close to Europa. Among the less promising families investigated, only the Halo family is described.

Thus, the proposed method to classify the regions of stability proceeds along the following lines. After computing the main families of planar periodic orbits, we first search for a variety of vertical bifurcations that occur at d:n-resonant orbits of a given family. Then, we continue each vertically bifurcated d:n-resonant family of 3-D periodic orbits and trace its stability behavior. A dense set of "critical" orbits where the stability of the corresponding d:n-resonant families change helps in defining global stability regions in phase space [18].

Periodic Orbit Families

According to the preceding methodology, we describe in this section the main planar families of periodic orbits which form the backbone of the stability regions and then proceed to the computation of the vertical bifurcation from these families, which allows the

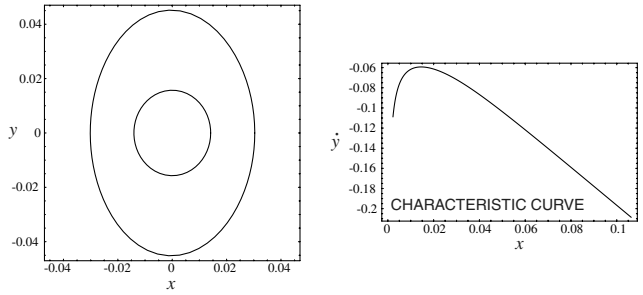

Fig. 1 Retrograde family of periodic orbits around Europa.

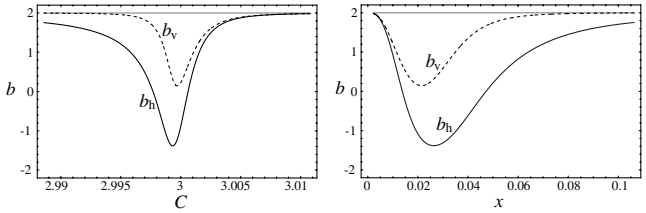

Fig. 2 C- and x_0-stability curves of the retrograde family.

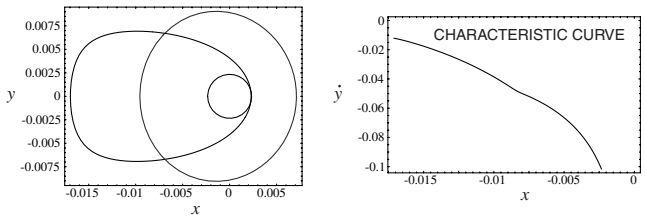

Fig. 3 Direct family of periodic orbits around Europa.

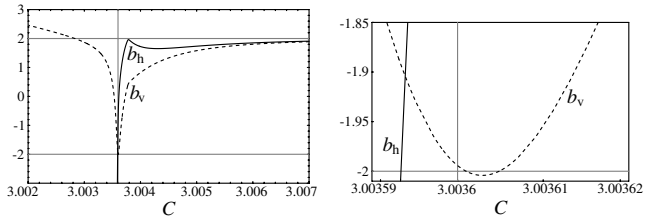

Fig. 4 Stability curves of the direct family.

estimation of the existence, the width, and the classification of stability regions.

Planar Families

Four planar families are considered, and all are formed by simple-periodic orbits. Two of the families, the retrograde and direct families, are the continuation of the families of circular orbits of the two-body problem to the CRTBP. The two other families are the Lyapunov families originating near the libration points L_1 and L_2.

Retrograde

The retrograde family starts with grazing retrograde equatorial orbits around Europa. For decreasing values of the Jacobi constant, the family continues with almost circular orbits of increasing size. Close to Hill's stability radius the orbits are no longer perturbed Keplerian ellipses around Europa, and consequently, its shape also changes in the rotating frame where we find near ellipses with the major axis in the y-axis direction and centered at Europa (see Fig. 1).

The orbits of the retrograde family are simple-periodic orbits that intersect the x axis perpendicularly. Therefore, initial conditions of any orbit of the retrograde family can be chosen such that $x = x_0$, $y = z = 0$, $\dot{x} = \dot{z} = 0$, and $\dot{y} = \dot{y}_0$. Thus, the totality of the retrograde family can be represented by a "characteristic curve" $\dot{y}_0 = \dot{y}_0(x_0)$ [14]. That is the convention used in the right plot of Fig. 1, where we note that the minimum velocity $v = 0.0593017$ occurs at a distance $r = 0.0145519$ units of length ($\approx$6.25 times the equatorial radius of Europa).

The left plot of Fig. 2 shows the stability curves (C, b) of Europa's retrograde family. In the right plot we show an analogous curve where abscissas are x_0 distances. All the orbits are linearly stable, and because neither b_h nor b_v take the critical values ± 2, we do not find any simple period or period doubling bifurcation of this family. However, we will see later that we can find vertical and horizontal bifurcations for different multiplicities of the period.

Direct

Starting from a planar equatorial direct periodic orbit close to Europa, we can continue the direct family. Figure 3 shows a portrait of the direct family that includes only nonimpact trajectories. The stability curves of the direct family are shown in Fig. 4.

Close to Europa, the orbits are low ellipticity ellipses centered at Europa with the major axis in the ordinates direction. Decreasing values of the Jacobi constant produce ellipses of increasing size. Both stability indices decrease slowly until the horizontal one reaches a relative minimum $b_h = 1.6515$ at $C = 3.00432$; the axes of the corresponding ellipse are $r_m = 0.00690716$, $r_M = 0.00722138$ ($r_m = 4631.51$, $r_M = 4842.21$ km). At this point, the shapes of the orbits change from low ellipticity ellipses to egg-shaped orbits with the basis towards Jupiter (direction of negative abscissas). The egg-shaped orbits become more and more exaggerated until impact with the surface of Europa at $C = 3.0036$ (vertical lines in Fig. 4). The evolution of this family for decreasing values of the Jacobi constant is similar to Darwin's "family A of satellites" [19] and Broucke's analogous family H_1 [20] (or Henon's g' family of the Hill problem [13]), with highly unstable orbits and passing through several collisions, that is not of interest for the subject of this paper. Note in the detail of Fig. 4 the two vertical period doubling bifurcations ($b_v = -2$) that occur close before the egg-shaped orbits impact Europa.

Other

Other families of planar orbits can be computed starting from small ellipses around the (unstable) collinear points [11]. The collinear points are placed in the x axis, at $x = 0.020485$ and $x = -0.020211$. We do not pay attention to the third collinear point. We call the L_2 family the family of planar periodic orbits that surround the collinear point L_2 (positive x). It exists for decreasing values of C. Figure 5 shows a portrait of the L_2 family that includes only nonimpact trajectories. The bottom-right plot of Fig. 5 shows

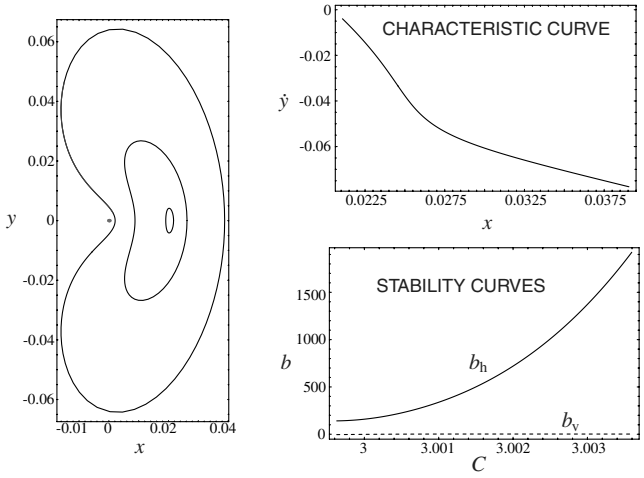

Fig. 5 Nonimpact orbits of the L_2 family.

the corresponding stability curves, where we note that all the orbits behave with high instability against in-plane perturbations ($|b_h| \gg 2$). In general, the orbits also present instability with respect to out-of-plane perturbations, but there is a small region where the vertical stability index is $|b_v| < 2$.

The orbits of the L_1 family are almost symmetric with respect to the y axis to those of the L_2 family, with a similar behavior.

Bifurcation to 3-D Motion

Following the proposed stability analysis, we now describe the vertical bifurcations of the previous planar families. The determination of the critical inclination at which the stable character of these families changes determines the boundary of the stability regions associated with the planar families. Change from instability to stability along a 3-D family indicates a 3-D stability region not necessarily connected with a region associated with a planar family. This is demonstrated, for example, in the case of the Halo family described at the end of this section.

Restrictions on the Bifurcation Order

We compute bifurcations of the previously computed families of planar periodic orbits for different multiplicities of the period by using Eq. (6). However, first of all we must note that not every resonance is always possible. That is the case of the retrograde family. As previously noted, we do not find simple period (1:1-resonance, $b = +2$) or period doubling (1:2-resonance, $b = -2$) bifurcations of the retrograde family. Furthermore, as appreciated in Fig. 2, the minimum value $b_{v,m} \approx 0.146$ of the vertical stability index limits the possible resonances to

$$\frac{d}{n} = \frac{1}{2\pi}\arccos\left(\frac{b_{v,m}}{2}\right) \approx \frac{41}{172} < \frac{1}{4}$$

On the contrary, we can find bifurcations on the plane farther away than the 1:4-resonance. However, the minimum value $b_{h,m} \approx -1.38$ of the horizontal stability index again limits the horizontal resonances that can occur to $d/n \approx 13/35$. Furthermore, because of these minima, we find two different bifurcations for each allowable d:n-resonance, except for exactly the value $b_{v,m}$ or $b_{h,m}$. For example, as appreciated in Fig. 2, $b_v = 1$ for both $C = 2.99871$ ($x_0 = 0.0349429$) and $C = 3.00107$ ($x_0 = 0.0114464$). Then, as derived from Eq. (6), we found two different 1:6-resonant orbits that give rise to two different families of 3-D periodic orbits that repeat themselves after $6 - 1 = 5$ crossings of the x–y plane in the upwards direction, or "cycles." This example is illustrated in Fig. 6 where we note that close to Europa (left plot) the orbit is almost circular remaining approximately between 7500 and 8000 km from Europa, whereas far away from Europa the orbit remains between 23,200 and 37,500 km from Europa (right plot).

Vertical Bifurcations of the Retrograde Family

To study the 3-D motion in a dense region around Europa we compute many families of 3-D periodic orbits bifurcated at different resonances. Some of them are detailed in the Appendix.

Following Hénon [13] we can find vertically bifurcated orbits with simple period at $x \neq 0$, $y = 0$, either with $z \neq 0$, $\dot{z} = 0$ (Hénon's type C_v) or with $z = 0$, $\dot{z} \neq 0$ (Hénon's type B_v). All the critical

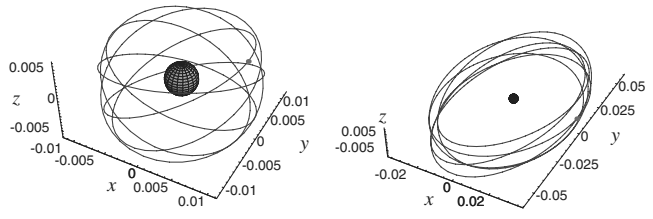

Fig. 6 Periodic orbits after five cycles close to and far away from Europa.

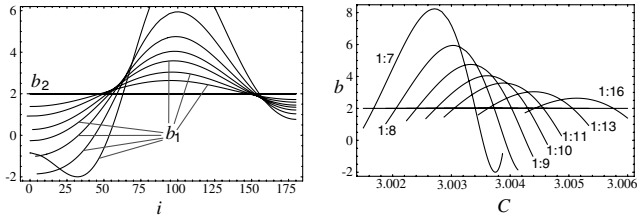

Fig. 7 The *i*- and *C*-stability curves of several resonant families close to Europa.

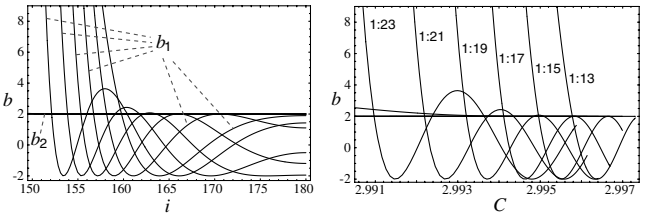

Fig. 8 The *i*- and *C*-stability curves of several resonant families far away from Europa.

orbits we computed are multiple periodic orbits, and we find both types of bifurcations.

Close to Europa, the families of 3-D periodic orbits show a typical behavior. Starting from a near circular equatorial retrograde periodic orbit that is resonant after n periods in the rotating frame and d rotations of Europa, a small perturbation either in the z (type C_v bifurcation) or in the $\dot{z}$ (type B_v bifurcation) directions produce a 3-D orbit that is periodic after $(n - d)$ cycles. Then, increasing values of the Jacobi constant produce 3-D orbits with decreasing inclination that evolve from retrograde to direct motion through the 180 deg of inclination.

Figure 7 presents the stability curves of several families close to Europa. As inclination angle, we use the inclination in degrees

$$i = \arctan(\dot{z}_0/\dot{y}_0) \tag{7}$$

of the velocity vector at the point $y_0 = z_0 = 0$, where $\dot{x}_0 = 0$. This angle provides a measure very similar to the averaged inclination for perturbed Keplerian ellipses and is an illustrative quantity for describing the evolution of non-Keplerian orbits. Note in Fig. 7 that, within the numerical precision, the index b_2 always takes the degenerate value $b_2 = +2$. This index is related to intrinsic displacements in the (instantaneous) out-of-plane direction with the result of some indefinition in the argument of the node in the rotating frame of the 3-D orbits.

Near circular orbits change their stability character at certain critical inclinations i_c, and for the computed families we find large areas of instability centered around polar orbits, yet slightly displaced to highly inclined retrograde orbits ($i \simeq 100$ deg). The changes in the stability properties of almost circular orbits are related to bifurcations of stable eccentric orbits. All these orbits form a single connected equatorial stability region near Europa.

Far away from Europa, d:n-resonant families exist for decreasing values of the Jacobi constant. In the rotating frame, the 3-D orbits remain approximately on the surface of an elliptic cylinder that increases its height for decreasing values of the Jacobi constant. The height of the cylinder is directly related to the velocity inclination Eq. (7) and at certain height/inclination the periodic orbits change to instability. The left plot of Fig. 8 presents the stability curves of several families far away from Europa in terms of the velocity inclination, where we note the abrupt change in orbit stability at certain critical inclinations. The minimum retrograde inclination for which the orbits are stable decreases for increasing distances to Europa. However, starting from the 1:19-resonance, a region of mild instability appears whose size increases with distance. This may

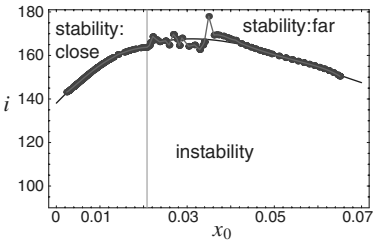

Fig. 9 Boundary of the region of strong instability around Europa.

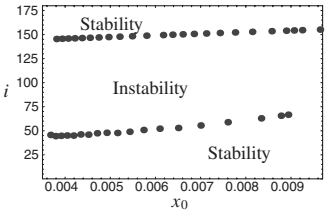

Fig. 10 Stability regions for almost circular motion close to Europa.

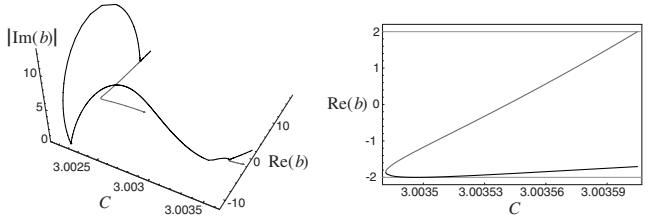

Fig. 11 Stability curves of the 1:2-resonant family of egg-shaped periodic orbits.

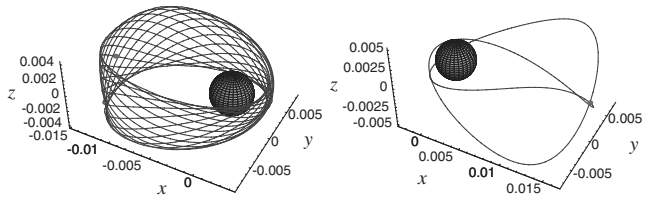

Fig. 12 Stable egg-shaped orbits. Left: 6:17 resonant. Right: 1:2 resonant.

indicate the existence of small stability regions disconnected from the main region centered around the DRO family. These regions have, however, the same qualitative characteristics as the main stable region noting that they contain members of the same families of periodic orbits.

By joining a dense set of points (x_0, i_c) corresponding to the different d:n-resonant families, we can obtain an estimate of the main stability regions in 3-D space as presented in Fig. 9, where the vertical axis marks the boundary $(d/n \approx 41/172)$ between resonances close to and far away from Europa. In the far away

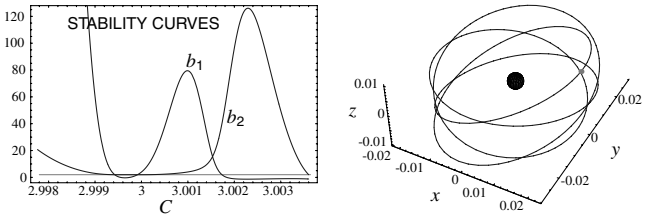

Fig. 13 Family bifurcated from the direct family and a sample stable orbit.

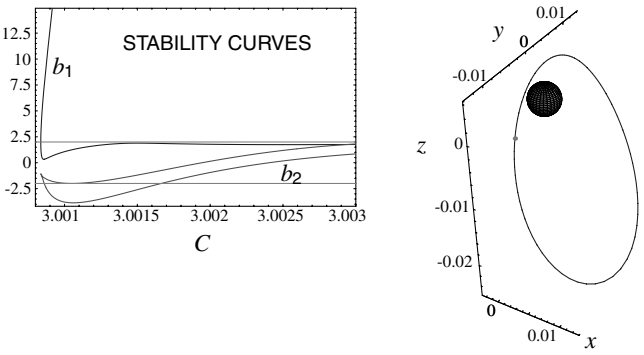

Fig. 14 Halo L_2 family and a sample stable orbit.

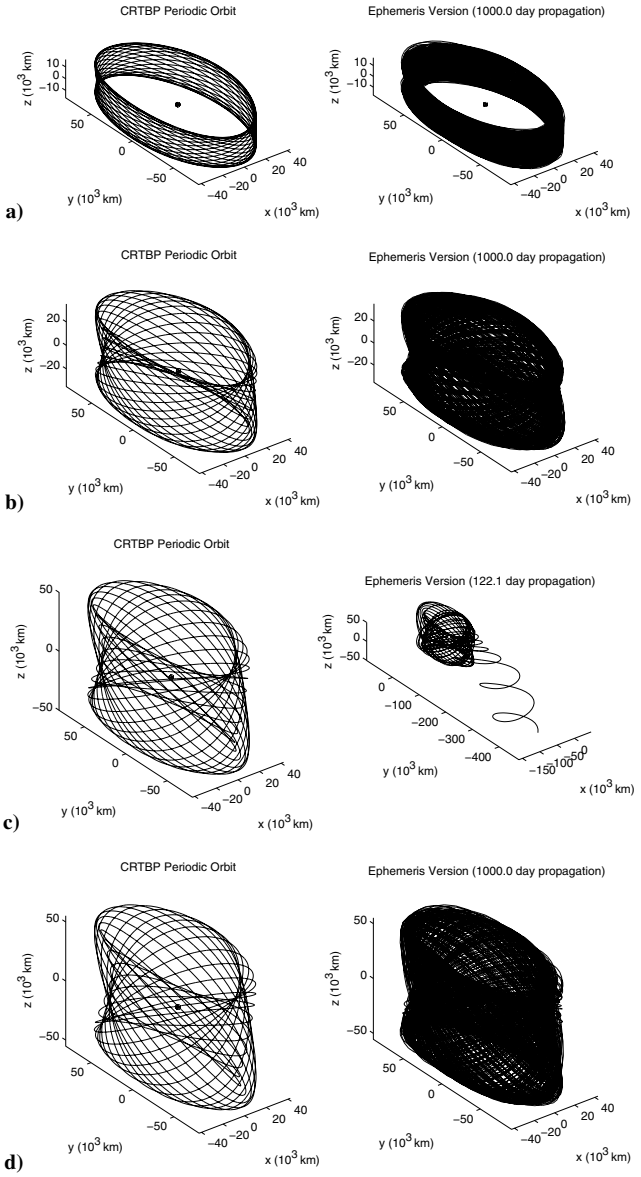

Fig. 15 Evolution of the 1:23 family of ephemeris model retrograde periodic orbits.

case the (x_0, i_c) points correspond to the change to strong instability. A least squares fit is superimposed on the points that mark the change in the stability of the 3-D periodic orbits.

Figure 9 is in good agreement with the "red sea plot" of Lam and Whiffen (see Fig. 14 of [8]) that presents a neck in the stability region between 14,000 and 24,000 km, approximately, corresponding to the

Table 1 Active bodies and gravitational parameters

Body	GM (km^3/s^2)	GM source	Position source
Io	5.959916033410404E + 03	JUP230	JUP230
Europa	3.202738774922892E + 03	JUP230	JUP230
Ganymede	9.887834453334144E + 03	JUP230	JUP230
Callisto	7.179289361397270E + 03	JUP230	JUP230
Jupiter	1.266865349218008E + 08	JUP230	JUP230
Saturn	3.794062976400000E + 07	JUP230	DE405
Uranus	5.794548600000000E + 06	JUP230	DE405
Neptune	6.836534900000000E + 06	JUP230	DE405
Sun	1.327132332402215E + 11	JUP230	DE405

Table 2 Nonzero spherical harmonic coefficients for the active bodies

Body	Term	Unnormalized value	Source
Europa	J2	4.355E − 04	Ref. [22]
Europa	C22	1.315E − 04	Ref. [22]
Jupiter	J2	1.469642900697847E − 02	JUP230
Jupiter	J3	−6.436411055625769E − 07	JUP230
Jupiter	J4	−5.871402915754995E − 04	JUP230
Jupiter	J6	3.425025517100406E − 05	JUP230

irregular area of Fig. 9 and with an abrupt minimum around 22,500 km corresponding to the peak at the 1:6 resonance in Fig. 9. Then, the narrow yellow region of [8] corresponding to orbital lifetimes of ≈25 days, can be fitted to the cubic

$$i_c = 138.097 + 2136.79x_0 - 45,831.7x_0^2 + 246,110x_0^3$$

The agreement between Fig. 9 and Lam and Whiffen's red sea plot deteriorates far away from Europa. Note, however, that both figures are not directly comparable, and we find much better agreement when considering long lifetime orbits of the CRTBP [21] instead of restricting to stable periodic orbits.

Vertical Biburcations of the Direct Family

Analogously to the case of retrograde orbits, a variety of d:n-resonant families can be computed from the direct family. However, as shown in Fig. 7, many of them have been already computed in the case of retrograde motion close to Europa and belong to the same equatorial stability region. Then, as before, we compute a set (x_0, i_c) of points that define a stability region for direct, almost circular, 3-D motion close to Europa. Figure 10 presents the complete picture for the stability properties for this type of orbits.

Note in Fig. 10 (see also in Fig. 7) the difference between the stability regions in the direct and retrograde case: Although the angle α between the orbit at the critical inclination i_c and the equatorial plane decreases with the distance to Europa for retrograde orbits ($\alpha = 180$ deg $- i_c$), it increases with distance for direct orbits ($\alpha = i_c$).

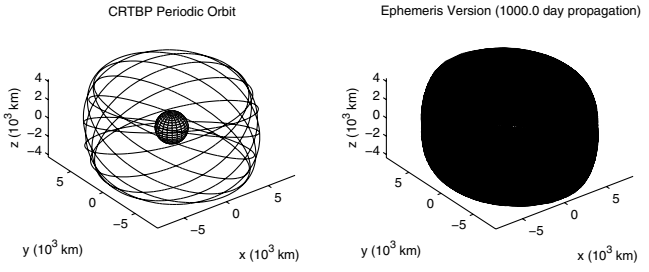

Fig. 16 Retrograde solution near the boundary of the stable DRO region.

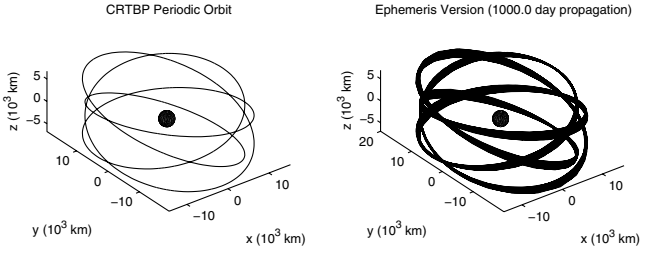

Fig. 17 Retrograde solution.

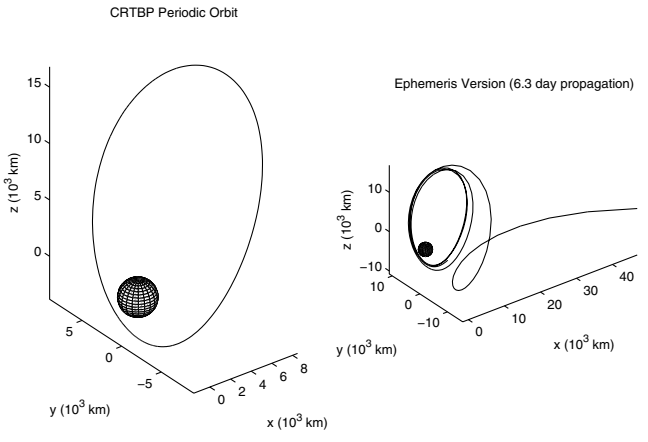

Fig. 18 Halo orbit stable in the CRTBP and unstable in the ephemeris model.

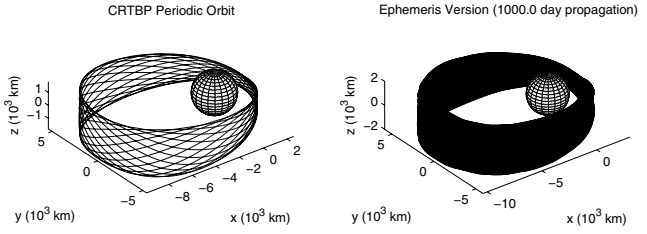

Fig. 19 Example direct egg-shaped orbit stable in the ephemeris model.

Table A1 44 vertical bifurcation resonant orbits of the equatorial retrograde family of the CRTBP close to Europa

d:n	x	$\dot{y}$	T	k_h
1:23	0.3826155041228084E − 02	−0.8526740864266236E − 01	0.2833375384917917E + 00	1.916645
1:22	0.395121985392241E − 02	−0.8410826617564759E − 01	0.2967692219374928E + 00	1.908514
1:21	0.4087028454079570E − 02	−0.8291796134798371E − 01	0.3115436314871053E + 00	1.899142
1:20	0.4235169389432638E − 02	−0.8169450285892589E − 01	0.3278737803889397E + 00	1.888264
1:19	0.4397531720600449E − 02	−0.8043572747028210E − 01	0.3460205352167187E + 00	1.875543
1:18	0.4576439877897677E − 02	−0.7913929251393015E − 01	0.3663069509926575E + 00	1.860539
1:17	0.4774777052176328E − 02	−0.7780267586322978E − 01	0.3891381319207067E + 00	1.842679
1:16	0.4996169162163832E − 02	−0.7642319031077169E − 01	0.4150292982030582E + 00	1.821195
1:15	0.5245248544734603E − 02	−0.7499802485045896E − 01	0.4446463540446393E + 00	1.795050
1:14	0.5528041807889960E − 02	−0.7352433578380875E − 01	0.4788660651113937E + 00	1.762808
1:13	0.5852557764653064E − 02	−0.7199943074351844E − 01	0.5188680602518417E + 00	1.722443
1:12	0.6229711060409965E − 02	−0.7042112944944802E − 01	0.5662805993161336E + 00	1.671029
2:23	0.6442585834317579E − 02	−0.6961157610440885E − 01	0.5934535710011006E + 00	1.639894
1:11	0.6674837113397634E − 02	−0.6878847155549984E − 01	0.6234216802580490E + 00	1.604212
2:21	0.6929498582707031E − 02	−0.6795211654087421E − 01	0.6566507878093163E + 00	1.563067
1:10	0.7210313224874694E − 02	−0.6710313814051030E − 01	0.6937195968865385E + 00	1.515310
2:19	0.7521965203620929E − 02	−0.6624264111146694E − 01	0.7353572832931125E + 00	1.459476
1:09	0.7870414158997231E − 02	−0.6537243691588972E − 01	0.7824979055137733E + 00	1.393679
2:17	0.8263391921073332E − 02	−0.6449539928279402E − 01	0.8363614496958487E + 00	1.315463
1:08	0.8711167909944450E − 02	−0.6361603394540601E − 01	0.8985789394543692E + 00	1.221586
3:23	0.9046852360368484E − 02	−0.6303184803246194E − 01	0.9457722554469952E + 00	1.148212
2:15	0.9227782626247681E − 02	−0.6274142865140307E − 01	0.9713924219179452E + 00	1.107700
3:22	0.9418498005530136E − 02	−0.6245274019643721E − 01	0.9985369409854700E + 00	1.064325
1:07	0.9833151434219369E − 02	−0.6188292069217829E − 01	0.1058008159074479E + 01	0.967878
3:20	0.1030009028276802E − 01	−0.6132830864874999E − 01	0.1125684848630590E + 01	0.856311
2:13	0.1055692893154534E − 01	−0.6105923085764407E − 01	0.1163209279870955E + 01	0.793876
3:19	0.1083190541690132E − 01	−0.6079742485591100E − 01	0.1203605734857834E + 01	0.726380
1:06	0.1144636611350280E − 01	−0.6030294133108111E − 01	0.1294651484142512E + 01	0.573927
4:23	0.1197685684557419E − 01	−0.5996743109372164E − 01	0.1374046774174339E + 01	0.441589
3:17	0.1216990502454047E − 01	−0.5986458802845467E − 01	0.1403106282203926E + 01	0.393497
2:11	0.1258484318004971E − 01	−0.5967592114004498E − 01	0.1465846672906467E + 01	0.290587
3:16	0.1304489475478843E − 01	−0.5951522777183572E − 01	0.1535822527217163E + 01	0.177707
4:21	0.1329500392154116E − 01	−0.5944790706816894E − 01	0.1574033119153793E + 01	0.117092
1:05	0.1414754818442209E − 01	−0.5931577338986633E − 01	0.1705062259033207E + 01	−0.084105
4:19	0.1521699626514246E − 01	−0.5934037032234122E − 01	0.1870811898885309E + 01	−0.320890
3:14	0.1564580518845134E − 01	−0.5940322748867374E − 01	0.1937594402971556E + 01	−0.409910
5:23	0.1602577653009806E − 01	−0.5948215937268645E − 01	0.1996883313977625E + 01	−0.485649
2:09	0.1667806482778222E − 01	−0.5966543432801284E − 01	0.2098836665591457E + 01	−0.608402
5:22	0.1747753426456767E − 01	−0.5996640285399415E − 01	0.2223934174440752E + 01	−0.745756
3:13	0.1814851772097931E − 01	−0.6027867857993052E − 01	0.2328886035791364E + 01	−0.849599
4:17	0.1933048745510534E − 01	−0.6094887675807979E − 01	0.2513222774023195E + 01	−1.007126
9:38	0.1994693483076238E − 01	−0.6135419221344066E − 01	0.2608872657482850E + 01	−1.076733
5:21	0.2079970106729542E − 01	−0.6197264163328550E − 01	0.2740373013495280E + 01	−1.159496
41:172	0.2133267537429230E − 01	−0.6239114754380821E − 01	0.2821960235195845E + 01	−1.203622

For almost circular direct motion we should limit to resonant families below the 1:6-resonance, where the orbits are clearly egg-shaped and the inclination information as defined in Eq. (7) must be used with care. The limit for d:n-resonant families of nonimpact direct egg-shaped 3-D periodic orbits is a period doubling bifurcation ($b_v = -2$) that occurs at $C = 3.003605$ (see the detail of Fig. 4). The stability curves of the corresponding family of periodic orbits is presented in Fig. 11.

For decreasing values of the Jacobi constant, the 3-D egg-shaped periodic orbits are stable until they change to instability at $C = 3.00348$ into a Krein collision of the eigenvalues, where the four nontrivial eigenvalues abandon the unit circle out of the real axis, and the stability indices take complex conjugated values. At $C = 3.00207$ the stability indices change to real. The family continues with unstable orbits until it suffers from a reflection at $C = 3.00205$. The rest of the family exists for increasing values of C and is made of unstable 3-D orbits that terminate at $C = 3.00253$ on a (highly unstable) planar orbit of a new family. The orbits of this new family are planar direct egg-shaped periodic orbits with the basis towards the positive x direction that are almost symmetric to the orbits of the previously computed egg-shape family and with an analogous behavior. We note, however, that the simply periodic egg-shape orbits with this orientation are also stable. We computed several 3-D periodic orbits bifurcated from the egg-shape families at different d:n-resonant orbits. Figure 12 shows an example. Thus it appears that the large stability region of direct equatorial orbits near Europa ends sharply as a stability region formed with higher-order egg-shape trajectories.

As appreciated in the detail of Fig. 4, there is another vertical period doubling bifurcation of the direct family at $C = 3.003601$. The stability curves of the corresponding bifurcated family are presented in the left plot of Fig. 13. This new family exists for decreasing values of the Jacobi constant with orbits of increasing size and inclination that, in general, are unstable. However, there is a narrow region of stability for $2.99943 < C < 2.99992$. The stable orbits show retrograde motion remaining at a distance between 8 and 15 radius of Europa, approximately, and with an inclination parameter $i \approx 165$ deg. These orbits thus connect to the stability regions associated with the DRO family.

Other Families

Despite the L_1 and L_2 families being highly unstable, we find two vertical bifurcations and continue the corresponding families of 3-D periodic orbits.

Thus, in reference to the L_2 family we find a vertical bifurcation at $C = 3.00094$ ($b_v = -2$) that produces eight-shaped orbits with increasing instability. The other vertical bifurcation occurs at $C = 3.00333$ ($b_v = +2$) and gives rise to the Halo family. The continuation of the Halo family to decreasing values of the Jacobi constant reaches a minimum at $C = 3.00084$ (see the left plot of

Table A2 44 vertical bifurcation resonant orbits of the equatorial retrograde family of the CRTBP far away from Europa

d:n	x	$\dot{y}$	T	k_h
1:23	0.6353941003776735E − 01	−0.1282527195536677E + 00	0.5886109062321278E + 01	0.979606
1:22	0.6250799648758544E − 01	−0.1263506882327820E + 00	0.5867551814766511E + 01	0.936367
1:21	0.6144038042188015E − 01	−0.1243862237302853E + 00	0.5847166767231673E + 01	0.889348
1:20	0.6033316664960482E − 01	−0.1223539227755164E + 00	0.5824668659952298E + 01	0.838041
1:19	0.5918241207212686E − 01	−0.1202475789617227E + 00	0.5799709296264242E + 01	0.781848
1:18	0.5798349459948331E − 01	−0.1180600054901806E + 00	0.5771859058725420E + 01	0.720057
1:17	0.5673093888800879E − 01	−0.1157828038360492E + 00	0.5740581452420173E + 01	0.651815
1:16	0.5541818013596126E − 01	−0.1134060564443594E + 00	0.5705197370513562E + 01	0.576099
1:15	0.5403723669442891E − 01	−0.1109179100941403E + 00	0.5664833835022133E + 01	0.491669
1:14	0.5257824436860801E − 01	−0.1083039974389727E + 00	0.5618348618540506E + 01	0.397016
1:13	0.5102877343660671E − 01	−0.1055466109709242E + 00	0.5564216150606297E + 01	0.290300
1:12	0.4937278975817452E − 01	−0.1026234829019499E + 00	0.5500348835196873E + 01	0.169268
2:23	0.4849847231578456E − 01	−0.1010911183208486E + 00	0.5463890424275696E + 01	0.102548
1:11	0.4758900261213762E − 01	−0.9950590666362791E − 01	0.5423805492824410E + 01	0.031180
2:21	0.4664044624656298E − 01	−0.9786275744273229E − 01	0.5379511649998888E + 01	−0.045265
1:10	0.4564808727934198E − 01	−0.9615568986027044E − 01	0.5330290902841109E + 01	−0.127248
2:19	0.4460619179881776E − 01	−0.9437758897042788E − 01	0.5275246210224154E + 01	−0.215258
1:09	0.4350767035328467E − 01	−0.9251986487884503E − 01	0.5213239387063441E + 01	−0.309796
2:17	0.4234358048347177E − 01	−0.9057196144060517E − 01	0.5142799767827626E + 01	−0.411350
1:08	0.4110236517985263E − 01	−0.8852062094221445E − 01	0.5061985114906921E + 01	−0.520346
3:23	0.4022465127732229E − 01	−0.8708735404640827E − 01	0.5001081789255903E + 01	−0.597292
2:15	0.3976863140197200E − 01	−0.8634873145297553E − 01	0.4968160512789386E + 01	−0.637063
3:22	0.3930004068751295E − 01	−0.8559424469954729E − 01	0.4933396357147299E + 01	−0.677693
1:07	0.3832107250811104E − 01	−0.8403341105503616E − 01	0.4857627165556660E + 01	−0.761473
3:20	0.3727806128222297E − 01	−0.8239488070964222E − 01	0.4772077094127238E + 01	−0.848416
2:13	0.3672865478619085E − 01	−0.8154257073309804E − 01	0.4724952716492553E + 01	−0.892950
3:19	0.3615802798079715E − 01	−0.8066564828086240E − 01	0.4674469719248956E + 01	−0.938088
1:06	0.3494285439023597E − 01	−0.7882807035097809E − 01	0.4561636930384047E + 01	−1.029699
4:23	0.3395345680098102E − 01	−0.7736402285143601E − 01	0.4464314754503994E + 01	−1.098887
3:17	0.3360582717701666E − 01	−0.7685689805782549E − 01	0.4428943829989498E + 01	−1.121877
2:11	0.3287929526380078E − 01	−0.7580986301805218E − 01	0.4353033836336723E + 01	−1.167484
3:16	0.3210440444511792E − 01	−0.7471313833378794E − 01	0.4269105948212905E + 01	−1.212195
4:21	0.3169566010781211E − 01	−0.7414333571927938E − 01	0.4223604145457339E + 01	−1.234023
1:05	0.3036237982477276E − 01	−0.7232907473034086E − 01	0.4069323294120554E + 01	−1.296036
4:19	0.2880506661070283E − 01	−0.7030301573492564E − 01	0.3878020147298908E + 01	−1.348824
3:14	0.2821209263677290E − 01	−0.6956017779018046E − 01	0.3802149426431286E + 01	−1.362809
5:23	0.2770024809963163E − 01	−0.6893249162873222E − 01	0.3735368228733427E + 01	−1.371975
2:09	0.2684926734310894E − 01	−0.6791797246249998E − 01	0.3621788175578199E + 01	−1.380937
5:22	0.2585007529673770E − 01	−0.6677581101439256E − 01	0.3484572346987732E + 01	−1.380780
3:13	0.2504538985568889E − 01	−0.6589709230384662E − 01	0.3371253241367818E + 01	−1.371594
4:17	0.2369569281198253E − 01	−0.6451235735145495E − 01	0.3176115797553956E + 01	−1.336141
9:38	0.2302319274726586E − 01	−0.6386723923684007E − 01	0.3076778119343246E + 01	−1.308181
5:21	0.2212553399144233E − 01	−0.6305635689305078E − 01	0.2942295105652748E + 01	−1.259089
41:172	0.2158269930150112E − 01	−0.6259553900765756E − 01	0.2860049250900922E + 01	−1.222396

Fig. 14) with a reflection in a small region of stable orbits. The orbits of the family continue with increasing values of C until they impact the surface of Europa at $C = 3.00108$. The right plot of Fig. 14 shows a stable orbit for $C = 3.00084$. Because of this small segment of stability on the stability curve of the Halo family, we expect a small stability region around these orbits to exist. The sample ephemeris integration below as well as the investigation of neighboring motion [9] show that this stability region is too small to persist in a more realistic model.

Because of symmetries in the model, we also find a symmetric solution with respect to the x–y plane. The behavior close to the L_1 point is almost symmetric to the L_2 case, and we do not give details here.

Ephemeris Runs

A sample of initial conditions are mapped from the CRTBP to a true ephemeris state at an arbitrary epoch to give an indication of the persistence, in a realistic model, of the stability regions found in the CRTBP. The ephemeris model is related to an epoch. However, because we are interested in long-term stability orbits, the epoch should be irrelevant to some extent, and we choose January 1, 2025 (Julian date of 2,460,677.0) for all our trials. The transformation uses average values, where the z axis is defined using the instantaneous Jupiter–Europa angular momentum, and the nominal value for the Europa–Jupiter distance is chosen to be 6.709×10^5 km, cf. p. 347 of [22].

The ephemeris model is based on three publicly available estimated solutions for the parameters, positions, velocities, and orientations of celestial bodies of interest. The JUP230 solution[§] provides the most recent estimate for the parameters and body states associated with the Jupiter system based on Galilean data. The DE405 solution[‖] [23] provides the body states for the barycenters of each of the major planets. The body orientation information is obtained via the pck00008.tpc file[¶] that is primarily based on the results from the International Astronomical Union/International Association of Geodesy (IAU/IAG) Working Group on Cartographic Coordinates and Rotational Elements of the Planets and Satellites in 2000 [24]. All three of the necessary files and readers are available from the spacecraft planet instrument c-matrix events (SPICE) information system created at the Jet Propulsion Laboratory.[**] The specific bodies and associated parameters used

[§]Data available online at ftp://naif.jpl.nasa.gov/pub/naif/generic_kernels/spk/satellites/jup230.bsp [cited 22 June 2005].

[‖]Data available online at ftp://naif.jpl.nasa.gov/pub/naif/generic_kernels/spk/planets/de405_2000-2050.bsp [cited 22 June 2005].

[¶]Data available online at ftp://naif.jpl.nasa.gov/pub/naif/generic_kernels/pck/pck00008.tpc [cited 22 June 2005].

[**]Data available online at http://naif.jpl.nasa.gov/naif/spiceconcept.html [cited 22 June 2005].

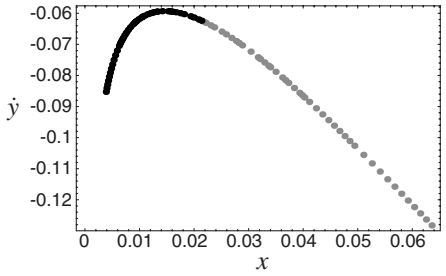

Fig. A1 Resonant orbits close to and further away from Europa.

for all ephemeris propagations in this study are included in Tables 1 and 2.

Figure 15 gives the evolution of the distant retrograde family of the 1:23 resonance via the integration of a sequence of sample members of the family. We observe that the lifetime of the orbits follows the stability curve of the family as was presented in Fig. 8. The orbit a on that figure is stable for at least 1000 days, the maximum time we use for our ephemeris computations. As the inclination increases the family moves towards the boundary of the stability region, case b, and enters a zone of mild instability evident from case c where the lifetime reduces to a few hundred days. Then, the family enters a narrow zone of stability confirmed by the 1000-day solution in case d, as is consistent with the left curve in Fig. 8.

Figures 16 and 17 give two examples of retrograde stable solutions; the first case, Fig. 16, is part of the 2:11 resonance family near the boundary of the stable DRO region. The second case, Fig. 17, corresponds to a retrograde orbit inside the small stability region of the family presented in Fig. 13. Although belonging to distinct families of periodic orbits, these trajectories belong to the same stability region. We observe that the path of these orbits share similar qualitative features.

Although the stability curves of Fig. 14 show that the Halo families do indeed have stable regions in the CRTBP, Fig. 18 indicates that this region appears to be too small to combat the perturbing forces introduced with a true ephemeris.

Finally, Fig. 19 gives an example of a direct orbit. The orbit of that figure is part of the egg-shaped family with resonance 6:17 also shown in Fig. 12. The orbit is generally stable, in the sense it reaches 1000-day lifetime.

Conclusions

The continuation of families of periodic orbits that bifurcate to three dimensions from families of planar periodic orbits of the circular restricted three-body problem allows us to determine different regions of long-term stability around Europa. Further, we described the mutual relations between different regions. The tests performed on a selected set of solutions using a real ephemeris model showed that nominal orbits robust to small perturbations indeed exist in the large stability regions. However, small segments of stability along a single family of the CRTBP may not be sufficient to ensure the existence of similar stable motion in an ephemeris model, as illustrated by the Halo family case. A study of neighboring motion thus appears to be necessary to complete the study of stability regions. This will be addressed in a subsequent paper.

We deal only with vertical bifurcations of the main families of planar orbits, paying special attention to the retrograde family, which provides large areas of long-term stability. However, the study of the horizontal bifurcations of the main families is left open, which will provide new families of planar orbits whose vertical bifurcations could lead to new stability regions.

Besides providing a map of the naturally occurring stability regions for use in spacecraft trajectory design, an unexpected and important result from this study is that, close to the primary, the stability region for direct orbits is larger than that for retrograde orbits. Thus, a direct orbit can handle a larger inclination and remain stable compared with the retrograde orbit.

Finally, it is important to note that the dynamical model and methods used in the paper are not restricted to space missions to Europa and generally apply to other high-science priority planetary satellites.

Appendix

Tables A1 and A2 provide the initial conditions of 88 families of periodic orbits that bifurcate vertically at 44 different resonances. As presented in Fig. A1, these resonances provide a dense set of points covering the part of the retrograde family in which we are interested in this work. Many other resonances closer to Europa were computed in [4].

Acknowledgements

Part of this work has been performed at the Jet Propulsion Laboratory, California Institute of Technology, under a contract with NASA. Martín Lara acknowledges partial support from the Spanish Government (project numbers ESP2004-04376 and ESP-2005-07107).

References

[1] Villac, B. F., and Aiello, J. J., "Mapping Long-Term Stability Regions Using the Fast Lyapunov Indicator," American Astronautical Society Paper 05-188, Jan. 2005.

[2] Johannesen, J. R., and D'Amario, L. A., "Europa Orbiter Mission Trajectory Design," *Advances in the Astronautical Sciences*, Vol. 103, No. 1, 1999, pp. 895–908.

[3] Scheeres, D. J., Guman, M. D., and Villac, B. F., "Stability Analysis of Planetary Satellite Orbiters: Application to the Europa Orbiter," *Journal of Guidance, Control, and Dynamics*, Vol. 24, No. 4, 2001, pp. 778–787.

[4] Lara, M., and San-Juan, J. F., "Dynamic Behavior of an Orbiter Around Europa." *Journal of Guidance, Control, and Dynamics*, Vol. 28, No. 2, 2005, pp. 291–297.

[5] San-Juan, J. F., Lara, M., and Ferrer, S., "Phase Space Structure Around Planetary Satellites," *Journal of Guidance, Control, and Dynamics*, Vol. 29, No. 1, 2006, pp. 113–120.

[6] Paskowitz, M. E., and Scheeres, D. J., "Orbit Mechanics About Planetary Satellites Including Higher Order Gravity Fields," American Astronautical Society Paper 2005-190, Jan. 2005.

[7] Whiffen, G., "A Preliminary Investigation of the Jupiter Icy Moon Orbiter," American Astronautical Society Paper 03-354, Aug. 2003.

[8] Lam, T., and Whiffen, G. J., "Exploration of Distant Retrograde Orbits Around Europa," American Astronautical Society Paper 05-110, Jan. 2005.

[9] Lara, M., Russell, R., and Villac, B., "On Parking Solutions Around Europa," American Astronautical Society Paper 05-384, Aug. 2005.

[10] Marzari, F., and Scholl, H., "On the Instability of Jupiter's Trojans," *Icarus*, Vol. 159, No. 2, 2002, pp. 328–338.

[11] Szebehely, V., *Theory of Orbits— The Restricted Problem of Three Bodies*, Academic Press, New York, 1967.

[12] Broucke, R., "Stability of Periodic Orbits in the Elliptic Restricted Three-Body Problem," *AIAA Journal*, Vol. 7, No. 6, 1969, pp. 1003–1009.

[13] Hénon, M., "Vertical Stability of Periodic Orbits in the Restricted Problem. II: Hill's case," *Astronomy and Astrophysics*, Vol. 30, No. 2, 1974, pp. 317–321.

[14] Hénon, M., "Exploration Numérique du Problème Restreint. II: Masses Égales, Stabilité des Orbites Périodiques," *Annales d'Astrophysique*, Vol. 28, No. 2, 1965, pp. 992–1007.

[15] Robin, I. A., and Markellos, V. V., "Numerical Determination of Three-dimensional Periodic Orbits Generated from Vertical Self-resonant Orbits," *Celestial Mechanics*, Vol. 21, No. 4, 1980, pp. 395–434.

[16] Davoust, E., and Broucke, R., "A Manifold of Periodic Orbits in the Planar General Three-body Problem with Equal Masses," *Astronomy and Astrophysics*, Vol. 112, No. 2, 1982, pp. 305–320.

[17] Deprit, A., and Henrard, J., "Natural Families of Periodic Orbits," *Astronomical Journal*, Vol. 72, No. 2, 1967, pp. 158–172.

[18] Lara, M., and Scheeres, D. J., "Stability Bounds for Three-Dimensional Motion Close to Asteroids," *Journal of the Astronautical Sciences*, Vol. 50, No. 4, 2002, pp. 389–409.

[19] Darwin, G. H., "Periodic Orbits," *Acta Mathematica*, Vol. 21, 1897,

pp. 99–243.
[20] Broucke, R. A., "Periodic Orbits in the Restricted Three-Body Problem With Earth-Moon Masses," NASA-JPL TR 32-1168, Feb. 1968, p. 71.
[21] Hénon, M., "Numerical Exploration of the Restricted Problem. VI: Hill's Case: Non-Periodic Orbits," *Astronomy and Astrophysics*, Vol. 9, No. 1, 1970, pp. 24–36.
[22] Bagenal, F., Dowling, T., and McKinnon, W., (eds.), *Jupiter, The Planet, Satellites, and Magnetosphere*, Cambridge Planetary Society, Cambridge, U.K., 2004, p. 285.
[23] Standish, E. M., *JPL Planetary and Lunar Ephemerides* [CD-ROM], Willman–Bell, Richmond, VA, 1997.
[24] Seidelmann, P. K., Abalakin, V. K., Bursa, M., Davies, M. E., de Bergh, C., Lieske, J. H., Oberst, J., Simon, J. L., Standish, E. M., Stooke, P., and Thomas, P. C., "Report of the IAU/IAG Working Group on Cartographic Coordinates and Rotational Elements of the Planets and Satellites: 2000," *Celestial Mechanics and Dynamical Astronomy*, Vol. 82, No. 1, 2002, pp. 83–111.